Clinical Chemistry 64:12
1762–1771 (2018)

Denaturation-Enhanced Droplet Digital PCR for Liquid Biopsies

Mariana Fitarelli-Kiehl,[1] Fangyan Yu,[1] Ravina Ashtaputre,[1] Ka Wai Leong,[1] Ioannis Ladas,[1] Julianna Supplee,[2] Cloud Paweletz,[2] Devarati Mitra,[1] Jonathan D. Schoenfeld,[1] Sareh Parangi,[3] and G. Mike Makrigiorgos[1*]

BACKGROUND: Although interest in droplet-digital PCR technology (ddPCR) for cell-free circulating DNA (cfDNA) analysis is burgeoning, the technology is compromised by subsampling errors and the few clinical targets that can be analyzed from limited input DNA. The paucity of starting material acts as a "glass ceiling" in liquid biopsies because, irrespective how analytically sensitive ddPCR techniques are, detection limits cannot be improved past DNA input limitations.

METHODS: We applied denaturation-enhanced ddPCR (dddPCR) using fragmented genomic DNA (gDNA) with defined mutations. We then tested dddPCR on cfDNA from volunteers and patients with cancer for commonly-used mutations. gDNA and cfDNA were tested with and without end repair before denaturation and digital PCR.

RESULTS: By applying complete denaturation of double-stranded DNA before ddPCR droplet formation the number of positive droplets increased. dddPCR using gDNA resulted in a 1.9–2.0-fold increase in data-positive droplets, whereas dddPCR applied on highly-fragmented cfDNA resulted in a 1.6–1.7-fold increase. End repair of cfDNA before denaturation enabled cfDNA to display a 1.9–2.0-fold increase in data-positive signals, similar to gDNA. Doubling of data-positive droplets doubled the number of potential ddPCR assays that could be conducted from a given DNA input and improved ddPCR precision for cfDNA mutation detection.

CONCLUSIONS: dddPCR is a simple and useful modification in ddPCR that enables extraction of more information from low-input clinical samples with minor change in protocols. It should be applicable to all ddPCR platforms for mutation detection and, potentially, for gene copy-number analysis in cancer and prenatal screening.

In the era of personalized medicine, molecular analysis of small-input clinical samples such as liquid biopsy–obtained circulating DNA are of great interest because of their broad potential as clinically significant biomarkers of disease. Although real-time PCR *(1–6)*, mutation/methylation enrichment *(7–16)*, and sequencing technologies *(17–20)* are widely used for detecting DNA alterations in liquid biopsies, interest in digital PCR *(21)* is rising rapidly in view of robust quantitative aspects of the technology and the emergence of commercial droplet-digital PCR (ddPCR)[4] platforms *(11, 22–25)*. ddPCR has been implemented in diverse fields such as cancer biomarkers *(26)*, viral load detection, prenatal screening, organ donor rejection, or library assessment for next generation sequencing *(27–29)*. Detection of emerging resistance or minimal residual disease via ddPCR in liquid biopsies is also growing *(30)*.

Despite progress, ddPCR technology is restricted by the inherent problems associated with limited number of input DNA copies available for analysis *(31)*. When just a few nanograms of circulating DNA are analyzed, the information obtained is affected by statistical sampling errors and the number of clinically relevant targets that can be analyzed is reduced. The paucity of starting material acts as a "glass ceiling" in liquid biopsies because, irrespective of how analytically sensitive ddPCR techniques are, detection limits cannot be improved past the DNA input limitations. Although preamplification of DNA can be applied to increase the material before

[1] Department of Radiation Oncology, Dana-Farber Cancer Institute and Brigham and Women's Hospital, Harvard Medical School, Boston, MA; [2] Department of Medical Oncology and Belfer Institute for Applied Cancer Science, Dana-Farber Cancer Institute, Harvard Medical School, Boston, MA; [3] Department of General & Gastrointestinal Surgery, Massachusetts General Hospital, Harvard Medical School, Boston, MA.
* Address correspondence to this author at: Dana Farber Cancer Institute, 450 Brookline Ave., Boston, MA 02115. Fax 617-525-7123; e-mail mike_makrigiorgos@dfci.harvard.edu.

Disclaimer: The contents of this manuscript do not necessarily represent the official views of the National Cancer Institute or the National Institutes of Health. The authors declare that all data supporting the findings of this study are available within the paper and its online Supplementary Information.

Received June 26, 2018; accepted September 4, 2018.
Previously published online at DOI: 10.1373/clinchem.2018.293845

[4] Nonstandard abbreviations: ddPCR, droplet-digital PCR; dsDNA, double-stranded DNA; dddPCR, denaturation-enhanced ddPCR; gDNA, genomic DNA; WT, wild type; ssDNA, single-stranded DNA; MT, mutant; SNP, single nucleotide polymorphism; RSE, relative standard error.

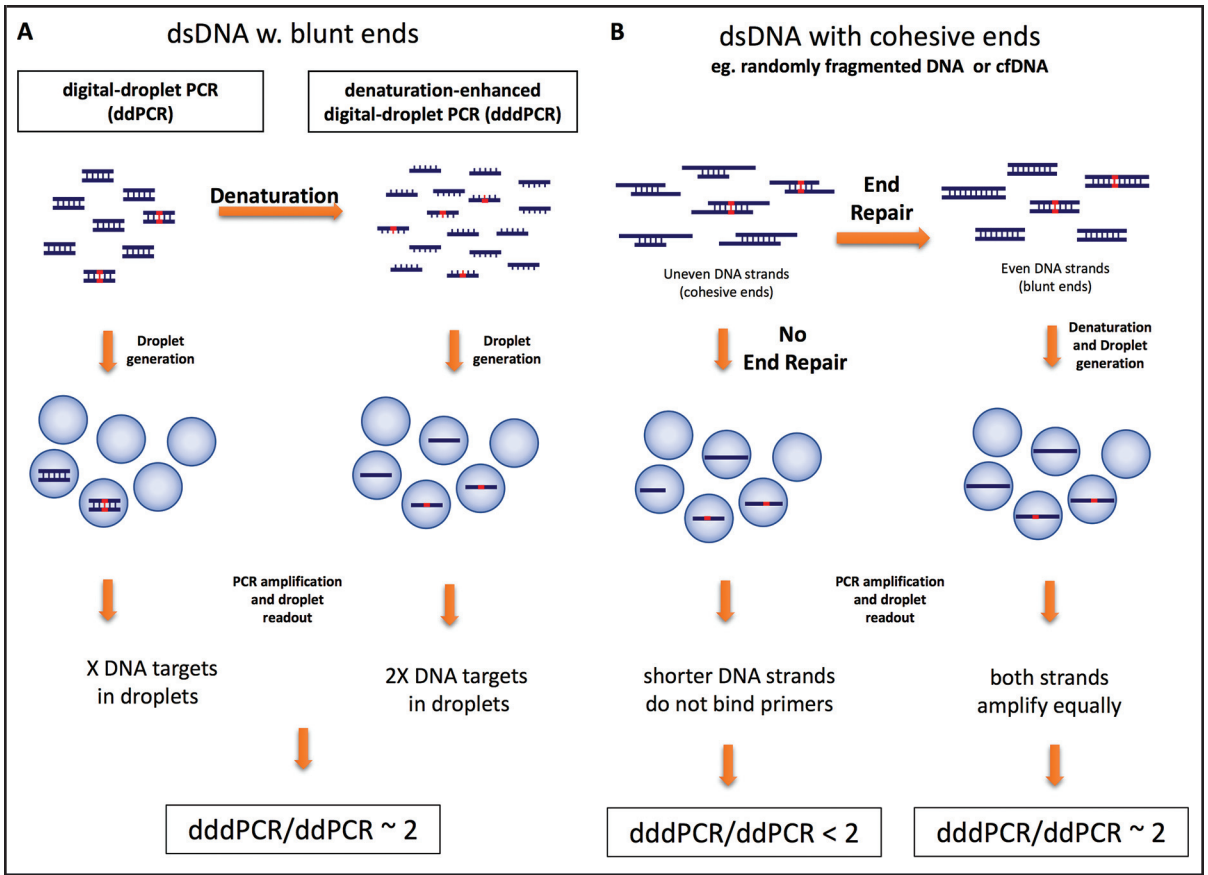

Fig. 1. Concept and workflow of dddPCR as compared to standard ddPCR.

dddPCR incorporates a DNA denaturation step prior to droplet generation (A). A mixture of fragmented gDNA, primers, hydrolysis probes, and ddPCR buffer is heated to denature the template, following which ssDNA molecules are partitioned into different droplets. Compared with standard ddPCR, data-positive droplets are doubled using dddPCR. Use of end repair to blunt the DNA strands in the case of circulating DNA (B). The 2 strands become blunted, leading to doubling of the positive droplets following dddPCR. Without end repair the ratio of dddPCR/ddPCR data-positive droplets is less than 2. End repair and denaturation are carried out sequentially in a single tube reaction. DNA fragments with red bases represent mutated DNA.

ddPCR, this spoils absolute quantification and introduces a number of additional experimental problems *(32)*.

Here we describe a simple approach to enhance the information obtained via digital PCR technology when analyzing limited-input DNA samples for mutations. As of its inception *(21)*, digital PCR amplifies individual double-stranded DNA (dsDNA) molecules in distinct reaction compartments, then obtains signal readout from each compartment to reveal and quantify DNA targets *(33)*. Yet the information contained in dsDNA is redundant because each mutated base appears in both sense and antisense strands of the original molecule. We therefore hypothesized that applying complete denaturation of dsDNA just before droplet formation in ddPCR would double the number of positive droplets obtained from a given DNA amount, thus enhancing ddPCR analysis of clinical samples. Indeed, amplification using just a sense or antisense DNA strand in a droplet is likely to produce the same number of positive droplets as the corresponding double-stranded molecule, provided the 2 strands are of equal size to begin with (blunt-ended DNA; Fig. 1A). Conversely, if the DNA is randomly fragmented with unequal strands, as in circulating DNA, then placing each strand in a separate droplet may not double the ddPCR signal because the shorter strand may not bind the primers. We demonstrate that a DNA end repair step performed just before denaturation and droplet formation restores the ability to double the ddPCR signal (Fig. 1B). This adaptation of digital PCR, denaturation-enhanced ddPCR (dddPCR), en-

Table 1. Sequences of primers and hydrolysis probes used for ddPCR and dddPCR.

Assay/mutation	Oligonucleotide ID	Sequence (5′-3′)	Amplicon length (bp)
BRAF p.V600E	BRAF-15-F2	AGACCTCACAGTAAAAATAGGT	83
	BRAF-15-R2	ACAACTGTTCAAACTGATGG	
	BRAF-WT	6FAM-TCTAGCTACAGTGAAATCTCGA-BHQ1[a]	
	BRAF-V600E-Mut	HEX-TCTAGCTACAGAGAAATCTCGA-BHQ1	
BRAF p.V600K	BRAF1–15-F1	TTTCTTCATGAAGACCTCACA	111
	BRAF2-R1	CCACAAAATGGATCCAGACAACTGT	
	BRAF-WT	6FAM-TCTAGCTACAGTGAAATCTCGA-BHQ1	
	BRAF-V600K-Mut	HEX-TCTAGCTACAAAGAAATCTCGAT-BHQ1	
NRAS p.Q61K	NRAS-3-F2	GTGAAACCTGTTTGTTGGA	79
	NRAS-3-R2	GTCCTCATGTATTGGTCTCT	
	NRAS-WT	6FAM-ACAGCTGGACAAGAAGAGTACA-BHQ1	
	NRAS-Q61K-Mut	HEX-ACAGCTGGAAAAGAAGAGTACA-BHQ1	
EGFR p.L858R	Forward primer	GCAGCATGTCAAGATCACAGATT	78
	Reverse primer	CCTCCTTCTGCATGGTATTCTTTCT	
	WT probe	VIC-AGTTTGGCCAGCCCAA-MGB-NFQ	
	MT probe	6FAM-AGTTTGGCCCGCCCAA-MGB-NFQ	

[a] BHQ1, Black Hole Quencher 1; NFQ, nonfluorescent quencher.

ables extraction of more information from small-input clinical samples without substantial changes in existing digital PCR protocols.

Materials and Methods

GENOMIC DNA AND CIRCULATING CELL-FREE DNA SAMPLES

Genomic DNA (gDNA) from cell-line MDA-MB-435S (HTB-129D, ATCC) and the Tru-Q1 Reference Standard (HD728, Horizon Discovery) were used as mutated DNA controls for B-Raf proto-oncogene, serine/threonine kinase (*BRAF*)[5] p.V600E and NRAS proto-oncogene, GTPase (*NRAS*) p.Q61K. Human male gDNA (G1471, Promega) was used as a wild type (WT) control and mixed with mutant DNA to create serially diluted samples. gDNA was digested before ddPCR reactions, using 10 U of *Hind*III-HF restriction enzyme (New England Biolabs) per 1 μg of gDNA according to manufacturer's instructions, with 15-min incubation at 37 °C.

Plasma and serum samples from patients with cancer and from healthy volunteers were obtained from Massachusetts General Hospital, Dana Farber Cancer Institute, and Brigham and Women's Hospital under consent and Institutional Review Boards approval. Blood from donors was collected with EDTA and then processed within 1 h of collection. Blood was first centrifuged at 1500–1800*g* for 20 min at room temperature. Plasma was then transferred to a 15-mL falcon tube and centrifuged a second time at 1500–1800*g* for 20 min at 4 °C. Supernatants were stored at −80 °C for further processing. Cell-free circulating DNA (cfDNA) was isolated from plasma and serum using the QIAamp MinElute Mini Kit or QIAamp Circulating Nucleic Acids Kit (Qiagen), and cfDNA was quantified on a Qubit 3.0 fluorometer using a dsDNA HS assay kit (Thermo Fisher Scientific).

DENATURATION-ENHANCED DIGITAL-DROPLET PCR

dddPCR without DNA end repair. A QX100 Droplet Digital PCR System (Bio-Rad) was used for detection of *BRAF* p.V600E, *BRAF* p.V600K, *NRAS* p.Q61K, and epidermal growth factor receptor (*EGFR*) p.L858R mutations. Primers and probe sequences were previously published *(12, 28, 34)* and are displayed in Table 1. The amplicon sizes were 78–111 bp for all assays. For each reaction, 1X ddPCR Supermix for probes (Bio-Rad) was mixed with 1 μmol/L forward and reverse primers, 250 nmol/L 6-FAM and HEX or VIC hydrolysis probes (IDT Technologies), and DNA template (5–30 ng of input) to a final volume of 20 μL, as recommended by Bio-Rad. The samples containing the reaction compo-

[5] Human genes: *BRAF*, B-Raf proto-oncogene, serine/threonine kinase; *NRAS*, NRAS proto-oncogene, GTPase; *EGFR*, epidermal growth factor receptor.

Table 2. Fold change of positive droplet concentration and RSE between samples analyzed by dddPCR and ddPCR.[a]

	Fold change (dddPCR/ddPCR)		RSE			
			ddPCR		dddPCR	
Sample	WT	MT	WT	MT	WT	MT
WT	1.9	N/A	0.077	N/A	0.056	N/A
MT 0.5%	1.9	1.8	0.086	1.161	0.062	0.870
MT 1%	1.9	2.1	0.082	0.793	0.059	0.545

[a] The concentration value (copies per microliter) for each sample represents 4 merged replicates, depicted in Fig. 2.

nents and DNA already mixed were placed in a Mastercycler Nexus Thermal Cycler (Eppendorf) for DNA denaturation at 95 °C for 1 min. The temperature was then reduced to 37 °C and the samples were loaded onto an 8-channel cartridge (Bio-Rad) along with 70 μL of droplet generation oil (Bio-Rad). Following emulsion generation on the QX100 Droplet Generator (Bio-Rad), the samples were transferred to a 96-well PCR plate, heat-sealed with foil, and amplified in a Mastercycler Nexus Thermal Cycler. The thermal cycling conditions comprised initial denaturation and polymerase activation for 10 min at 95 °C, followed by 50 cycles of 94 °C for 30 s and 56 °C for 1 min, enzyme deactivation at 98 °C for 10 min, and infinite hold at 10 °C. Alternatively, to decrease the chance of single-stranded DNA (ssDNA) damage by prolonged heating, a modified cycling protocol comprising 2 min of preactivation at 95 °C followed by 3 cycles of PCR, for generating dsDNA before proceeding to full polymerase activation at 95 °C for 10 min and 50 cycles of amplification.

Regular ddPCR was performed in parallel for each sample using the same cycling conditions described above but omitting DNA denaturation before droplet generation. The fluorescence signal for each probe was simultaneously measured by QX100 Droplet Reader (Bio-Rad) and results were analyzed with QuantaSoft™ v.1.3.2.0 software.

dddPCR with DNA end repair for cfDNA. In preliminary experiments, cfDNA end repair to produce blunt ends was performed as follows: 150 ng of cfDNA was treated with 1X NEBNext® Ultra™ II End Prep Enzyme Mix in 1X NEBNext Ultra II End Prep Reaction Buffer (New England Biolabs) in a total of 60 μL of reaction. Tris-HCl 10mM was added to complete the total volume and the samples were incubated at 20 °C for 30 min and 65 °C for 30 min as recommended by the manufacturer. The end-repaired cfDNA was purified with the QIAquick PCR Purification Kit (Qiagen) and then 1–10 ng of purified end-repaired cfDNA was used either for dddPCR or for standard ddPCR reactions as described above.

Subsequently, a homogeneous single-tube protocol was developed. Five nanograms of extracted cfDNA was mixed with 10 μL of 2X ddPCR Supermix for probes (Bio-Rad) and 0.5 μL of 20X NEBNext Ultra II End Prep Enzyme Mix was added in a total of 17.9 μL reaction. The mixture was incubated at 20 °C for 30 min for end repair and 65 °C for 30 min for enzyme inactivation; then 1 μmol/L forward and reverse primers and 250 nmol/L 6-FAM and HEX or VIC hydrolysis probes (for *BRAF* p.V600E and *EGFR* p.L858R) or 1X TaqMan® single-nucleotide polymorphism (SNP) Genotyping Assay for *EGFR* rs1050171 (ThermoFisher) were added, completing the final 20-μL volume. The samples were denatured at 95 °C for 1 min for dddPCR denaturation, cooled down to 37 °C, and then proceeded to droplet generation. Thermo-cycling conditions were as described previously. Experiments using cfDNA were repeated on independent days, with at least 3 replicas each time. dddPCR and ddPCR experiments were performed in parallel, and no-enzyme controls for cfDNA and gDNA were routinely included.

STATISTICAL ANALYSIS

Results were reported as copies per μL of reaction, determined by the QuantaSoft software (Bio-Rad). Error bars represent the 95% CI using Poisson distribution. For merged wells, the outer bars represent the standard error of the mean for the replicates and the inner ones are the Poisson error bars. The relative standard error (RSE; Table 2) was calculated by dividing the square root of the concentration value by the concentration estimate. The Welch *t*-test (2-tailed, unpaired) was applied for comparison between groups of droplets. Statistical analysis was performed with GraphPad Prism7.

Results

dddPCR APPLIED ON gDNA

Single-target analysis. In preliminary experiments, gDNA digested with a restriction enzyme was used to analyze the

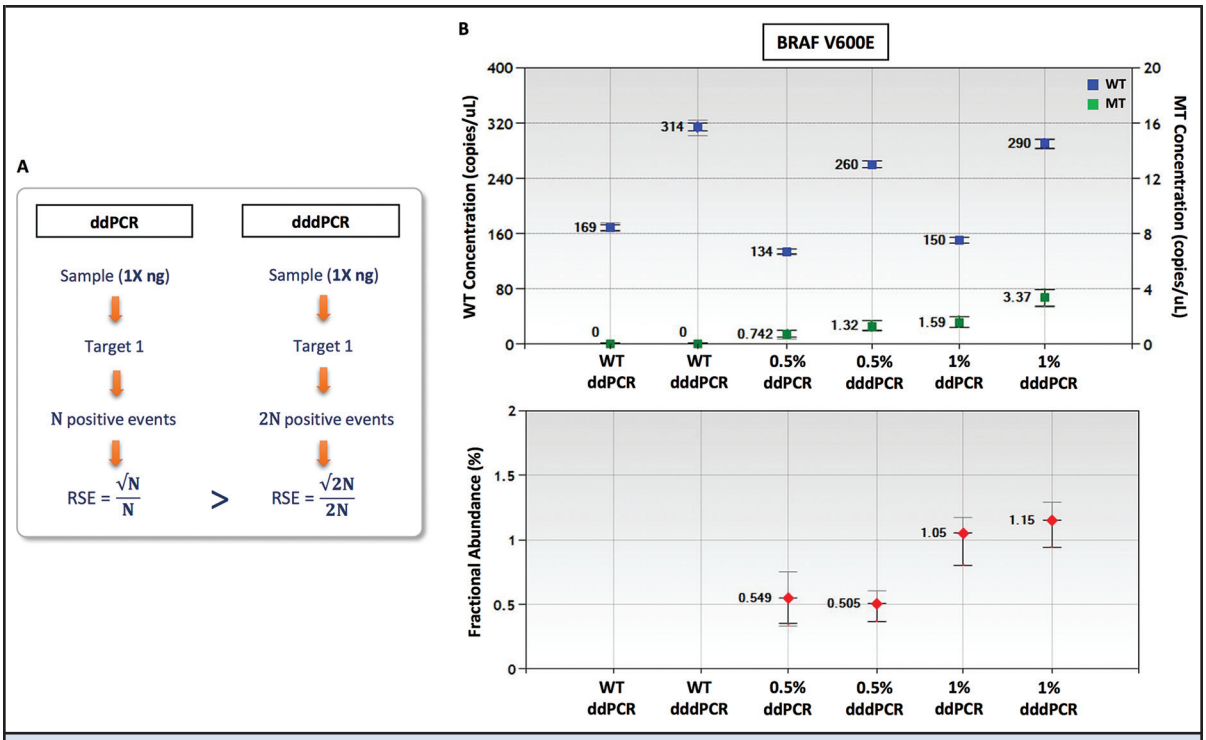

Fig. 2. For a given DNA input, the number of positive events using dddPCR is twice that of ddPCR, thus improving the RSE in the analysis.
Demonstration of the concept. (B), ddPCR and dddPCR for *BRAF* V600E using 10 ng of HTB-19 cell line gDNA serially diluted into WT DNA (A). Outer bars represent the standard error of the mean for the replicates; the inner error bar is the 95% CI for the Poisson distribution. Each sample is composed of 4 merged replicates.

effect of DNA denaturation before droplet formation. We employed dddPCR on 5 ng of gDNA containing 5% *BRAF* p.V600E mutation abundance and using hydrolysis TaqMan probes that distinguished the mutation from WT DNA. Compared with standard ddPCR, no difference in the clustering pattern on the 2D-plots was observed (see Fig. 1A in the Data Supplement that accompanies the online version of this article at http://www.clinchem.org/content/vol64/issue12), whereas the number of WT and mutant positive events approximately doubled using dddPCR (see Fig. 1B in the online Data Supplement). In control experiments, WT samples were also subjected to 2 or 3 consecutive rounds of the denaturation protocol, 1 min of denaturation followed by cooling to 37 °C, before droplet formation (see Fig. 1C in the online Data Supplement). This was done to investigate whether the increase in the positive events was due in part to polymerase synthesis following partial activation of the "hot-start" polymerase. If polymerase synthesis occurred following the first denaturation step, then additional rounds of denaturation before droplet generation would be expected to cause proportional increase in the positive events. However, the number of positive events was similar for 1 to 3 rounds of denaturation (see Fig. 1, B and D in the online Data Supplement), indicating that the doubling of data points was related to denaturation and segregation of ssDNA into droplets and not to amplification before droplet partitioning.

Next, dddPCR and standard ddPCR were applied to 10 ng of gDNA harboring *BRAF* p.V600E mutation at 1% and 0.5% allele fractions. The samples were run in quadruplicate, following the workflow depicted in Fig. 2A. The number of copies per microliter of reaction and the fractional abundance for the merged replicates are shown in Fig. 2B, and the values for individual replicates are shown in Fig. 2 in the online Data Supplement. The fold change of the copies per microliter, calculated by dividing the merged copies per microliter values of dddPCR by the values of ddPCR, ranged from 1.8–2.1-fold (Table 2), indicating that DNA was fully denatured before droplet formation in the dddPCR protocol. Moreover, the calculated RSE of concentration for WT and mutant (MT) copies was smaller for dddPCR than for standard ddPCR (Table 2), thus improving measurement accuracy.

In dddPCR, DNA is denatured and ssDNA molecules are partitioned into droplets. Thus, the measured concentration reflects the number of ssDNA copies. Accordingly, to quantify the original gDNA input, the con-

centration values should be divided by 2. We compared the WT and MT copies per microliter values of gDNA samples analyzed by standard ddPCR with the concentration values divided by 2 for samples analyzed by dddPCR. There was no significant difference between the 2 methods (see Fig. 3 in the online Data Supplement). Thus, if gDNA is fully denatured before droplet generation and the concentration values derived by the current commercial software are divided by 2, the absolute quantification is preserved using dddPCR.

Prolonged exposure of DNA to increased temperatures, in Tris-EDTA buffer, could lead to DNA damage, introducing bias in ddPCR measurements, although damage is not significant in the commercial ddPCR mastermix *(35)*. As a precaution, we implemented a modified cycling protocol applied after droplet generation that included 2 min polymerase preactivation at 95 °C followed by 3 cycles of PCR to generate dsDNA before proceeding with the regular protocols of 10 min of activation at 95 °C and 50 cycles of PCR. This modified protocol was compared side by side with the standard cycling for both ddPCR and dddPCR and the results were found to be equivalent (see Fig. 4 in the online Data Supplement). The modified protocol was adopted for further experiments.

Next, dddPCR and ddPCR were applied to gDNA containing *BRAF* p.V600E mutation at 10% allelic fraction at DNA input of 10, 5, 2.5, and 1.25 ng. The fold change in concentration (copies per microliter) as obtained by dividing dddPCR values by ddPCR values was not significantly different across various gDNA input amounts (see Fig. 5, A and B in the online Data Supplement), indicating that dddPCR can be applied with variable input DNA quantities.

Analysis of 2 targets with half the initial input each. Because dddPCR can double the number of positive events for a gDNA sample when compared to ddPCR, it should be possible to split the original sample in 2 reactions, thereby analyzing 2 different targets independently, each target resulting in similar number of positive droplets as a ddPCR applied on the entire sample (Fig. 3A). To test this assumption, we used HD728 gDNA reference mutation standard that contains *BRAF* p.V600E (8% allelic frequency) and *NRAS* p.Q61K (5% allelic frequency) and serially diluted this 1:5-, 1:20-, and 1:50-fold into WT gDNA. Fifteen nanograms DNA was used for dddPCR and 30 ng DNA for standard ddPCR. The number of positive events and the concentration of WT and MT copies obtained were similar for both dddPCR and ddPCR (Fig. 3B). Further, the resulting fractional mutation abundance was similar between protocols for all dilutions tested. Although caution would be required when splitting samples that contain just 1–2 copies of mutated alleles, the data indicate that, in general, samples can be interrogated for 2 mutations by dddPCR using the same quantity of DNA needed for analysis of only one mutation by standard ddPCR. Therefore, the number of potential assays is doubled by replacing ddPCR with dddPCR.

dddPCR APPLIED ON cfDNA FROM CLINICAL SAMPLES

cfDNA samples from patients with cancer previously screened for mutations were comparatively analyzed by dddPCR and ddPCR. Samples 13-post and 148-post represent plasma collected from 2 patients with cancer post-treatment and harbor *BRAF* p.V600K and p.V600E, respectively. Samples SCR, C8, and C11 represent plasma collected at 3 different chemotherapy treatment cycles from a single patient that harbor *EGFR* p.L858R and have a relatively low amount of cfDNA collected from plasma. WT cfDNA samples obtained from healthy donors were run in parallel as controls for all assays. The results are summarized in Fig. 6 and Table 1 in the online Data Supplement.

For 2 out of 5 cfDNA samples tested, there was increased confidence in calling a mutation when dddPCR was applied instead of standard ddPCR. For example, the 95% confidence limits for sample 13-post did not overlap with the WT control limits when analyzed via dddPCR (see Table 1 and Fig. 6A in the online Data Supplement). In contrast, there was overlap in confidence limits using standard ddPCR. Similar results are also shown for sample 148-post (see Table 1 and Fig. 6B in the online Data Supplement). These data demonstrate the higher discriminatory power of using dddPCR over ddPCR.

Across all cfDNA clinical samples tested, an increased number of positive droplets was obtained when applying dddPCR as opposed to ddPCR on cfDNA. However, the ratio of dddPCR/ddPCR copies per microliter was in the range 1.5–1.8 rather than 1.9–2.0 observed for gDNA. In view of this, an additional step was developed to increase further the positive events obtained with dddPCR for cfDNA (see below).

dddPCR APPLIED TO END-REPAIRED cfDNA

We hypothesized that when randomly fragmented, small-size DNA (e.g., cfDNA) was denatured and partitioned in droplets, some ssDNA copies could bind the PCR primers whereas others would not due to their size. Consequently, dddPCR would not result in doubling of positive droplets when compared to ddPCR. To enable application of dddPCR on randomly fragmented cfDNA while retaining a ratio of 1.9–2.0, like that obtained with large-fragment gDNA or blunt ended DNA, we added an end repair step before denaturation.

dddPCR using the current protocol was first applied multiple times on WT cfDNA obtained from healthy volunteers to obtain a dddPCR/ddPCR ratio baseline for nonrepaired cfDNA. *BRAF* p.V600E dddPCR assay was applied to 10, 3, and 1 ng WT cfDNA and the concen-

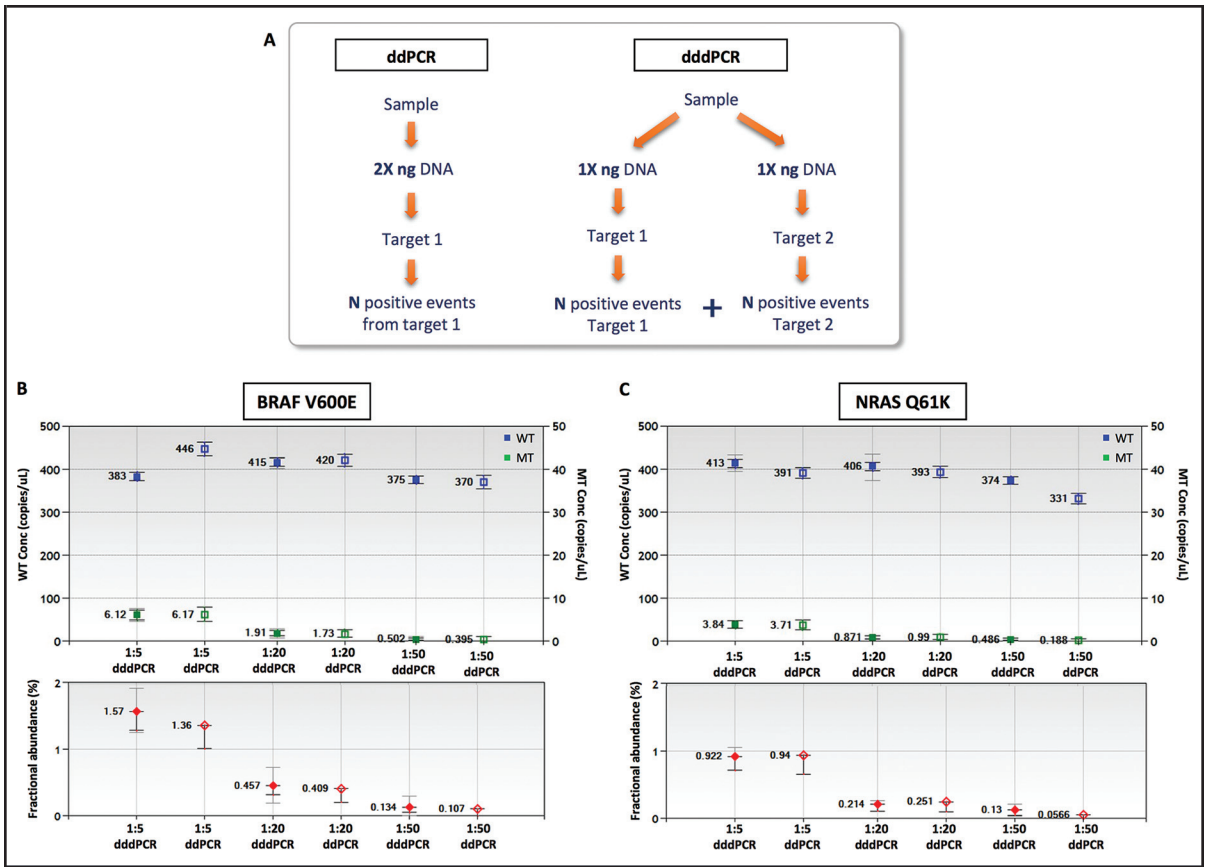

Fig. 3. dddPCR allows the analysis of 2 different targets in independent reactions using the same quantity of DNA used for a single ddPCR reaction and producing similar number of WT and MT copies in each reaction.

Demonstration of the concept (A). Analysis of gDNA HD728 serially diluted in WT DNA using 30 ng (ddPCR, nondenatured), or split in two 15-ng samples (dddPCR, denatured) as DNA input: *BRAF* V600E and *NRAS* Q61K screened, respectively (B) and (C). Undiluted gDNA HD728 contains *BRAF* V600E and *NRAS* Q61K mutations at 8% and 5% allelic frequencies, respectively. Error bars represent the 95% CI for the Poisson distribution. The dddPCR results represent merged wells for 2 replicates. The concentration of WT and MT copies obtained were similar for both dddPCR and ddPCR (for WT, $P = 0.49$, 0.71, and 0.69 for 1:5, 1:20, and 1:50 dilutions, respectively. For MT, $P = 0.79$, 0.34, and 0.19, respectively. The differences are not significant).

tration of copy numbers was compared to standard ddPCR (Fig. 4A). The mean ratio dddPCR/ddPCR copies per microliter was1.65 irrespective of the initial input, lower than 1.9–2.0 observed for gDNA (Fig. 4B). We also applied ddPCR and dddPCR protocols for additional ddPCR assays, designed to interrogate mutations *BRAF* p.V600K, *EGFR* p.L858R, and *EGFR* polymorphism rs1050171, which employed amplicons 78–111 bp and similar results were obtained (data not shown). Overall, in the absence of end repair, the ratio of dddPCR to ddPCR for cfDNA was about 1.65 for amplicon sizes of 78–111 bp in length that are used frequently.

Next, we performed end repair on WT cfDNA samples just before denaturation and droplet formation. Initially cfDNA was blunted with end-repair enzyme in the manufacturer-supplied buffer. The blunted cfDNA was then purified and analyzed via ddPCR or dddPCR in parallel, using 2 different assays, *BRAF* p.V600E and *EGFR* p.L858R (see Supplementary Fig. 7, A and B in the online Data Supplement). For both assays, the concentration fold change for end-repaired cfDNA was higher than for not-repaired cfDNA and, like gDNA, approximately 1.9–2.0 (see Fig. 7C in the online Data Supplement).

Subsequently, a single-tube, homogeneous protocol for end repair and dddPCR, described earlier in the Materials and Methods section, was developed by adding the end-repair enzyme directly into the ddPCR buffer. The single-tube end-repair dddPCR protocol was applied to 5 ng cfDNA using 2 different assays, *BRAF* p.V600E and *EGFR* SNP rs1050171. The concentration fold change

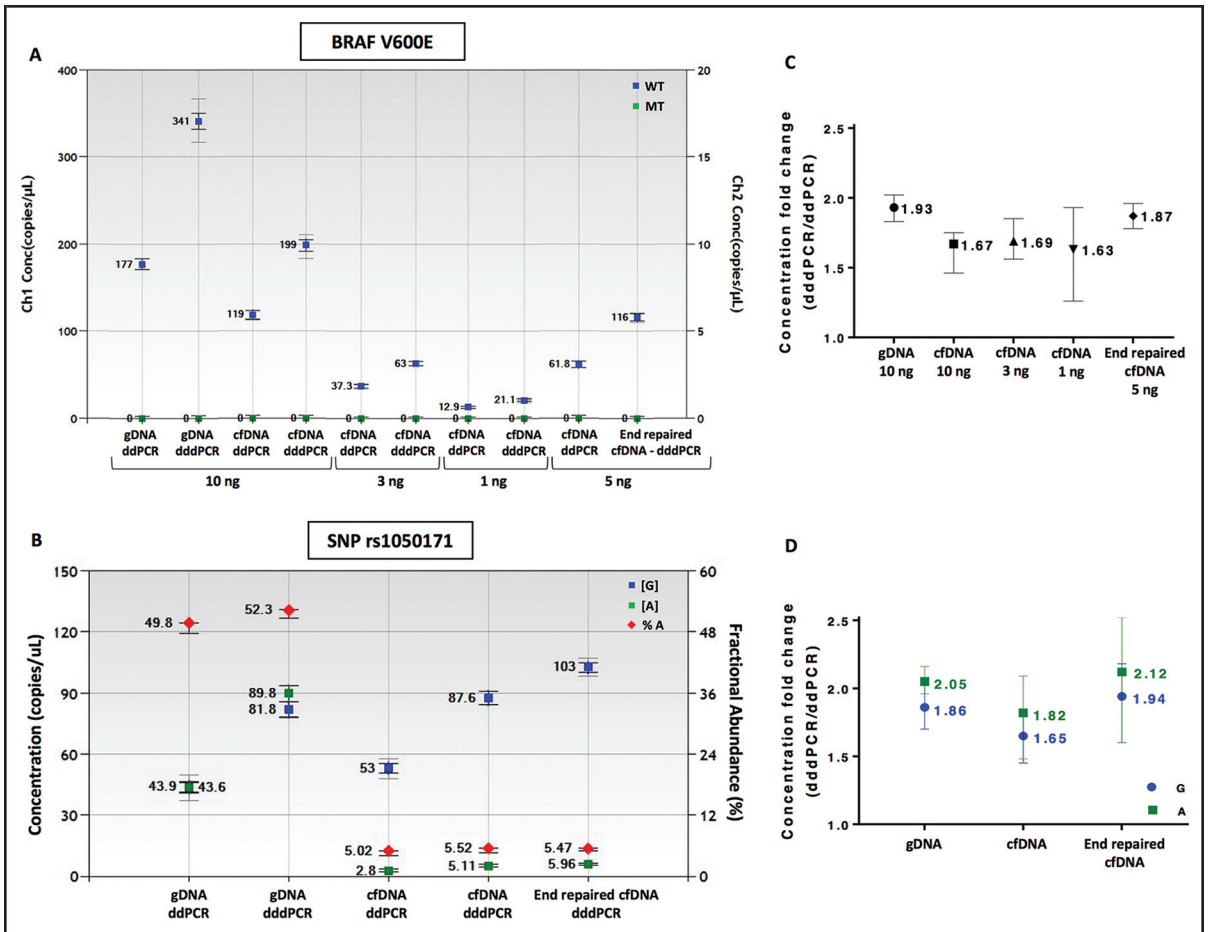

Fig. 4. dddPCR applied to randomly fragmented cfDNA and end-repaired cfDNA.

Comparison between number of copies per µL of reaction obtained by ddPCR and dddPCR using a *BRAF* V600E assay (A). Different input of WT cfDNA and 5-ng input of end-repaired cfDNA were analyzed along with WT gDNA as control. SNP rs1050171 assay was used to perform end repair followed by dddPCR, using cfDNA with 5% of allele A (B). The blue symbols represent copies with nucleotide G; green symbols are copies with nucleotide A; red symbols represent fractional abundance of allele A. The concentration fold change was calculated by dividing dddPCR by ddPCR values (C, D). End repair and dddPCR were performed sequentially in a single tube reaction. The error bars represent the range of fold change among replicas.

was obtained by dividing the end-repair dddPCR values by standard ddPCR values (Fig. 4). The *BRAF* assay was tested using WT cfDNA, resulting in an increased fold change for blunted cfDNA of 1.9–2.0, similar to gDNA (Fig. 4, A and C). A SNP rs1050171 assay was then used to test the end-repair dddPCR protocol on cfDNA. A cfDNA sample with 5% minority allele was prepared and the concentration fold change was compared for repaired vs nonrepaired cfDNA. gDNA (G1471), heterozygous for the same G/A polymorphism, was analyzed in parallel (Fig. 4B, D). Similar fold changes were observed for the 5% variant (allele A) and the 95% variant (allele G) for each condition, showing that by applying end repair to cfDNA the ratio of dddPCR to ddPCR was restored to 1.9–2.0, equal to that obtained for large fragments of gDNA or blunt DNA.

Discussion

The limited amount of DNA obtained from liquid biopsies restricts the number of targets that can be examined via ddPCR or real-time PCR and reduces the ability to identify rare mutations *(25, 36)*. It is possible to apply a DNA preamplification step before mutation detection and ddPCR to increase the material available *(29, 32)*. However, preamplification eliminates one of the main advantages of digital PCR, the absolute quantification of DNA copies, and the possibility for polymerase-introduced errors

increases. Further, preamplification may introduce measurement bias and decrease the precision of digital PCR *(32)* and entails an extra step that increases cost, complexity, and the risk for cross-contamination.

Applying complete denaturation just before droplet formation, as proposed in this work, entails minimal change to the established protocols and doubles the number of positive droplets without reducing the advantages of digital PCR. The benefit of this approach is to enable interrogation and precise quantification of lower percentage mutants than possible using standard ddPCR approaches with limited-mass material. Another benefit is the ability to split the sample and perform 2 digital PCR reactions examining different targets, while retaining the same number of droplets in each reaction. Increasing the targets that can be examined in ddPCR may also be achieved via amplitude multiplexing *(32)*. However, dddPCR is relatively simple and no major modifications of existing procedures are required, providing an almost no-cost approach to double the input DNA available for analysis. Unlike multiplexed ddPCR, in dddPCR there is no need for equipment with multiple optical channels, software for analysis of complex data, or extensive optimization. Moreover, dddPCR can be combined with existing multiplexing methods, thus enabling a single duplex ddPCR reaction to become 2 duplex dddPCR reactions, and so forth.

For cfDNA, an additional end repair step is applied to equalize sense and antisense strands and retain the approximate doubling of positive events following denaturation. This single-tube process entails direct addition of repair enzymes into the ddPCR mastermix. Although end repair performed in the same tube is a minor change to the overall protocol and is likely to result in better quantification, it is also possible to simply omit repair and apply a 1.6–1.7-fold increase in the number of positive droplets, as opposed to 1.9- to 2.0-fold obtained after repair, for cfDNA and amplicons between 70–110 bp in length. Thus, for absolute quantification purposes, a correction of 1.65-fold in the measured copy number concentration could be applied without cfDNA repair and a 1.95-fold can be applied with repair or whenever PCR amplicons are substantially smaller than the interrogated DNA fragments. Because of the proof-of-principle nature of this investigation, these values should be regarded as preliminary and additional studies must be conducted to finalize the corrections for optimal quantification.

Partial denaturation before droplet formation is considered to be a potential problem in ddPCR, because it might affect quantification *(27)*, and DNA damage in long templates may reduce the obtained number of positive events *(35, 37)*. As Figs. 1–4 demonstrate, these concerns are overcome using the current cycling protocol that enables complete denaturation and short (<110 bp) amplicons, while restricting excessive heating at 95 °C.

Although here we focus on droplet-based digital PCR, the same approach should be applicable to other digital PCR platforms. Further, although emphasis in this work is on mutations, doubling the number of positive droplets in digital PCR may be equally beneficial for copy number and gene amplification analysis via digital PCR *(38)*, because increasing the number of events decreases the overall measurement uncertainty. In addition to applications in cancer, dddPCR application in prenatal diagnosis or in organ transplantation can also be envisioned.

In summary, we developed a process for approximately doubling the number of positive events during ddPCR by partitioning denatured single DNA strands in droplets and by applying end repair before denaturation for the specific case of randomly fragmented DNA (cfDNA). This simple and useful modification doubles the potential number of assays from a given amount of input DNA and improves the confidence limits in digital PCR–based mutation detection. The process entails minor departure from established digital-PCR protocols and enables extraction of more information from precious clinical samples and liquid biopsies.

Author Contributions: *All authors confirmed they have contributed to the intellectual content of this paper and have met the following 4 requirements: (a) significant contributions to the conception and design, acquisition of data, or analysis and interpretation of data; (b) drafting or revising the article for intellectual content; (c) final approval of the published article; and (d) agreement to be accountable for all aspects of the article thus ensuring that questions related to the accuracy or integrity of any part of the article are appropriately investigated and resolved.*

M. Fitarelli-Kiehl and G.M. Makrigiorgos designed the experiments and prepared the manuscript. M. Fitarelli-Kiehl, F. Yu, R. Ashtaputre, K.W. Leong, I. Ladas, J. Supplee, and C. Paweletz contributed to the design and conduct of the experiments. D. Mitra, J.D. Schoenfeld, and S. Parangi provided clinical considerations. G.M. Makrigiorgos originated the development and supervised the study.

Authors' Disclosures or Potential Conflicts of Interest: *Upon manuscript submission, all authors completed the author disclosure form. Disclosures and/or potential conflicts of interest:*

Employment or Leadership: None declared.
Consultant or Advisory Role: None declared.
Stock Ownership: None declared.
Honoraria: None declared.
Research Funding: G.M. Makrigiorgos, National Institutes of Health grants R33 CA217652 and R01 CA221874 to the Dana Farber Cancer Institute.
Expert Testimony: None declared.
Patents: None declared.

Role of Sponsor: The funding organizations played a direct role in the design of study, choice of enrolled patients, review and interpretation of data, preparation of manuscript, and final approval of manuscript.

References

1. Tyagi S, Kramer FR. Molecular beacons: probes that fluoresce upon hybridization. Nat Biotechnol 1996;14: 303–8.
2. Bernard PS, Wittwer CT. Real-time PCR technology for cancer diagnostics. Clin Chem 2002;48:1178–85.
3. Li J, Wang F, Mamon H, Kulke MH, Harris L, Maher E, et al. Antiprimer quenching-based real-time PCR and its application to the analysis of clinical cancer samples. Clin Chem 2006;52:624–33.
4. Amicarelli G, Shehi E, Makrigiorgos GM, Adlerstein D. FLAG assay as a novel method for real-time signal generation during PCR: application to detection and genotyping of KRAS codon 12 mutations. Nucleic Acids Res 2007;35:e131.
5. Li J, Wang L, Janne PA, Makrigiorgos GM. Coamplification at lower denaturation temperature-PCR increases mutation-detection selectivity of TaqMan-based real-time PCR. Clin Chem 2009;55:748–56.
6. Sanchez JA, Pierce KE, Rice JE, Wangh LJ. Linear-after-the-exponential (LATE)-PCR: an advanced method of asymmetric PCR and its uses in quantitative real-time analysis. Proc Natl Acad Sci USA 2004;101:1933–8.
7. Li J, Wang L, Mamon H, Kulke MH, Berbeco R, Makrigiorgos GM. Replacing PCR with COLD-PCR enriches variant DNA sequences and redefines the sensitivity of genetic testing. Nat Med 2008;14:579–84.
8. Milbury CA, Li J, Makrigiorgos GM. Ice-COLD-PCR enables rapid amplification and robust enrichment for low-abundance unknown DNA mutations. Nucleic Acids Res 2011;39:e2.
9. How Kit A, Mazaleyrat N, Daunay A, Nielsen HM, Terris B, Tost J. Sensitive detection of KRAS mutations using enhanced-ice-COLD-PCR mutation enrichment and direct sequence identification. Hum Mutat 2013;34: 1568–80.
10. Liu Y, Song C, Ladas I, Fitarelli-Kiehl M, Makrigiorgos GM. Methylation-sensitive enrichment of minor DNA alleles using a double-strand DNA-specific nuclease. Nucleic Acids Res 2017;45:e39.
11. Hindson CM, Chevillet JR, Briggs HA, Gallichotte EN, Ruf IK, Hindson BJ, et al. Absolute quantification by droplet digital PCR versus analog real-time PCR. Nat Methods 2013;10:1003–5.
12. Song C, Liu Y, Fontana R, Makrigiorgos A, Mamon H, Kulke MH, Makrigiorgos GM. Elimination of unaltered DNA in mixed clinical samples via nuclease-assisted minor-allele enrichment. Nucleic Acids Res 2016;44: e146.
13. Ladas I, Yu F, Leong KW, Fitarelli-Kiehl M, Song C, Ashtaputre R, et al. Enhanced detection of microsatellite instability using pre-PCR elimination of wild-type DNA homo-polymers in tissue and liquid biopsies. Nucleic Acids Res 2018;46:e74.
14. Wu LR, Chen SX, Wu Y, Patel AA, Zhang DY. Multiplexed enrichment of rare DNA variants via sequence-selective and temperature-robust amplification. Nat Biomed Eng 2017;1:714–23.
15. Li J, Milbury CA, Li C, Makrigiorgos GM. Two-round coamplification at lower denaturation temperature-PCR (COLD-PCR)-based sanger sequencing identifies a novel spectrum of low-level mutations in lung adenocarcinoma. Hum Mutat 2009;30:1583–90.
16. Ladas I, Fitarelli-Kiehl M, Song C, Adalsteinsson VA, Parsons HA, Lin NU, et al. Multiplexed elimination of wild-type DNA and high-resolution melting prior to targeted resequencing of liquid biopsies. Clin Chem 2017;63: 1605–13.
17. Adalsteinsson VA, Ha G, Freeman SS, Choudhury AD, Stover DG, Parsons HA, et al. Scalable whole-exome sequencing of cell-free DNA reveals high concordance with metastatic tumors. Nat Commun 2017;8:1324.
18. Thomas RK, Nickerson E, Simons JF, Janne PA, Tengs T, Yuza Y, et al. Sensitive mutation detection in heterogeneous cancer specimens by massively parallel picoliter reactor sequencing. Nat Med 2006;12:852–5.
19. Milbury CA, Correll M, Quackenbush J, Rubio R, Makrigiorgos GM. COLD-PCR enrichment of rare cancer mutations prior to targeted amplicon resequencing. Clin Chem 2012;58:580–9.
20. Narayan A, Carriero NJ, Gettinger SN, Kluytenaar J, Kozak KR, Yock TI, et al. Ultrasensitive measurement of hotspot mutations in tumor DNA in blood using error-suppressed multiplexed deep sequencing. Cancer Res 2012;72:3492–8.
21. Vogelstein B, Kinzler KW. Digital PCR. Proc Natl Acad Sci USA 1999;96:9236–41.
22. Taly V, Pekin D, Benhaim L, Kotsopoulos SK, Le Corre D, Li X, et al. Multiplex picodroplet digital PCR to detect KRAS mutations in circulating DNA from the plasma of colorectal cancer patients. Clin Chem 2013;59: 1722–31.
23. Day E, Dear PH, McCaughan F. Digital PCR strategies in the development and analysis of molecular biomarkers for personalized medicine. Methods 2013;59:101–7.
24. Castellanos-Rizaldos E, Paweletz C, Song C, Oxnard GR, Mamon H, Janne PA, Makrigiorgos GM. Enhanced ratio of signals enables digital mutation scanning for rare allele detection. J Mol Diagn 2015;17:284–92.
25. Huggett JF, Cowen S, Foy CA. Considerations for digital PCR as an accurate molecular diagnostic tool. Clin Chem 2015;61:79–88.
26. Laurent-Puig P, Pekin D, Normand C, Kotsopoulos SK, Nizard P, Perez-Toralla K, et al. Clinical relevance of KRAS-mutated subclones detected with picodroplet digital PCR in advanced colorectal cancer treated with anti-EGFR therapy. Clin Cancer Res 2015;21:1087–97.
27. Huggett JF, Foy CA, Benes V, Emslie K, Garson JA, Haynes R, et al. The digital MIQE guidelines: Minimum Information for Publication of Quantitative Digital PCR Experiments. Clin Chem 2013;59:892–902.
28. Oxnard GR, Paweletz CP, Kuang Y, Mach SL, O'Connell A, Messineo MM, et al. Noninvasive detection of response and resistance in EGFR-mutant lung cancer using quantitative next-generation genotyping of cell-free plasma DNA. Clin Cancer Res 2014.
29. Murphy DM, Bejar R, Stevenson K, Neuberg D, Shi Y, Cubrich C, et al. NRAS mutations with low allele burden have independent prognostic significance for patients with lower risk myelodysplastic syndromes. Leukemia 2013;27:2077–81.
30. Diehl F, Schmidt K, Choti MA, Romans K, Goodman S, Li M, et al. Circulating mutant DNA to assess tumor dynamics. Nat Med 2008;14:985–90.
31. Postel M, Roosen A, Laurent-Puig P, Taly V, Wang-Renault SF. Droplet-based digital PCR and next generation sequencing for monitoring circulating tumor DNA: a cancer diagnostic perspective. Expert Rev Mol Diagn 2018;18:7–17.
32. Whale AS, Cowen S, Foy CA, Huggett JF. Methods for applying accurate digital PCR analysis on low copy DNA samples. PLoS One 2013;8:e58177.
33. Hindson BJ, Ness KD, Masquelier DA, Belgrader P, Heredia NJ, Makarewicz AJ, et al. High-throughput droplet digital PCR system for absolute quantitation of DNA copy number. Anal Chem 2011;83:8604–10.
34. Herrmann MG, Durtschi JD, Bromley LK, Wittwer CT, Voelkerding KV. Amplicon DNA melting analysis for mutation scanning and genotyping: cross-platform comparison of instruments and dyes. Clin Chem 2006; 52:494–503.
35. Bhat S, McLaughlin JL, Emslie KR. Effect of sustained elevated temperature prior to amplification on template copy number estimation using digital polymerase chain reaction. Analyst 2011;136:724–32.
36. Milbury CA, Li J, Makrigiorgos GM. PCR-based methods for the enrichment of minority alleles and mutations. Clin Chem 2009;55:632–40.
37. Bhat S, Curach N, Mostyn T, Bains GS, Griffiths KR, Emslie KR. Comparison of methods for accurate quantification of DNA mass concentration with traceability to the international system of units. Anal Chem 2010;82: 7185–92.
38. Gevensleben H, Garcia-Murillas I, Graeser MK, Schiavon G, Osin P, Parton M, et al. Noninvasive detection of HER2 amplification with plasma DNA digital PCR. Clin Cancer Res 2013;19:3276–84.